DFT and TDDFT Study Related to Electron Transfer in Nonbonded Porphine···C_{60} Complexes

Teemu L. J. Toivonen,*,† Terttu I. Hukka,† Oana Cramariuc,†,‡ Tapio T. Rantala,‡ and Helge Lemmetyinen†

Institute of Materials Chemistry, Tampere University of Technology, P.O. Box 541, 33101 Tampere, Finland, and Institute of Physics, Tampere University of Technology, P.O. Box 692, 33101 Tampere, Finland

Received: April 6, 2006; In Final Form: June 1, 2006

Spectroscopic properties of a ground state nonbonded porphine−buckminsterfullerene (H_2P···C_{60}) complex are studied in several different relative orientations of C_{60} with respect to the porphine plane by using the density functional (DFT) and time-dependent density functional (TDDFT) theories. The geometries and electronic structures of the ground states are optimized with the B3LYP and PBE functionals and a SVP basis set. Excitation energies and oscillator strengths are obtained from the TDDFT calculations. The relative orientation of C_{60} is found to affect the equilibrium distance between H_2P and C_{60} especially in the case of the PBE functional. The excitation energies of different H_2P···C_{60} complexes are found to be practically the same for the same excitations when the B3LYP functional is used but to differ notably when PBE is used in calculations. Existence of the states related to a photoinduced electron transfer within a porphyrin−fullerene dyad is also studied. All calculations predict a formation of an excited charge-transfer complex state, a locally excited donor (porphine) state, as well as a locally excited acceptor (fullerene) state in the investigated H_2P···C_{60} complexes.

I. Introduction

Understanding of the photochemical processes, which involve a photoinduced electron transfer in dyads, is important when designing artificial photosynthetic systems that mimic the natural photosynthesis and also when developing molecular electronic devices from these systems. Knowledge of the effects of a particular orientation and a certain distance between a donor and an acceptor on electron-transfer properties is essential for designing dyads, which harvest solar energy in an efficient manner and are capable of forming a charge-separated state and thereby an electrochemical potential.

Fullerenes[1,2] are good electron acceptors because they have the ability to accept multiple electrons,[3] and the reorganization energies in electron-transfer reactions in which fullerenes are involved are small.[4] When a donor-acceptor dyad containing fullerene is designed for operating in the visible spectral region, an electron donor that is capable of absorbing light at visible wavelengths is needed. Porphyrins have strong absorption bands in the visible region of the spectrum[5] and are capable of transferring the photoinduced charge and their excitation energy to a fullerene acceptor.[6−8]

The generalized kinetic scheme that is used in modeling the photodynamics of porphyrin−fullerene dyads is presented in Figure 1.[8] The scheme consists of the following nine main steps. (1) The ground state (PC) is excited to a locally excited second singlet state of porphyrin ($P^{2S}C$). (2) $P^{2S}C$ relaxes into the energetically lower, locally excited first singlet state of porphyrin ($P^{1S}C$). (3) $P^{1S}C$ may relax either directly to an exciplex ((PC)*) or (4) via a locally excited singlet state of fullerene (PC^{1S}) (5) to an exciplex that then (6) finally relaxes via a complete charge-separated state (P^+C^-) back (7) to the ground state. (8) The PC^{1S} state may also relax via the locally excited triplet state of fullerene (PC^{1T}) (9) to the ground state. In our work, only singlet excited states are considered as having also been studied in almost all of the experimental procedures.

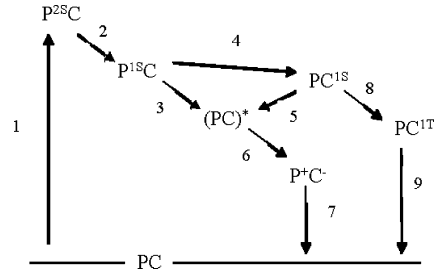

Figure 1. Generalized kinetic scheme used in modeling of the photophysical processes of porphyrin−fullerene dyads.[8] The energy levels are not drawn to scale. The states shown are the ground state (PC), locally excited singlet states of porphyrin ($P^{2S}C$ and $P^{1S}C$), excited charge-transfer complex state ((PC)*)), locally excited singlet state of fullerene (PC^{1S}), locally excited triplet state of fullerene (PC^{1T}), and the complete charge-separated state (P^+C^-).

In this study, the spectroscopic properties of a complex composed of a free base porphyrin (porphine), H_2P, and a buckminsterfullerene, C_{60}, have been investigated with the electronic structure calculations. The molecular structure of the studied complex is presented in Figure 2. These molecules were selected for computational modeling without chemical linkers because experimental observations of complete charge-separated state and the formation of an exciplex in covalently bonded porphyrin−fullerene dyads[8] raise the question as to whether these states can also be found by using theoretical methods for similar but structurally simpler systems.

In modeling of interaction, the orientation of C_{60} with respect to the molecular plane of H_2P was especially taken into account.

* Corresponding author. E-mail: teemu.toivonen@tut.fi.
† Institute of Materials Chemistry.
‡ Institute of Physics.

10.1021/jp062156c CCC: $33.50
Published on Web 10/18/2006

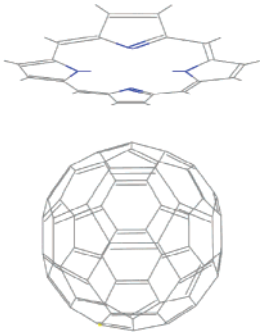

Figure 2. Molecular structure of a porphine−fullerene complex.

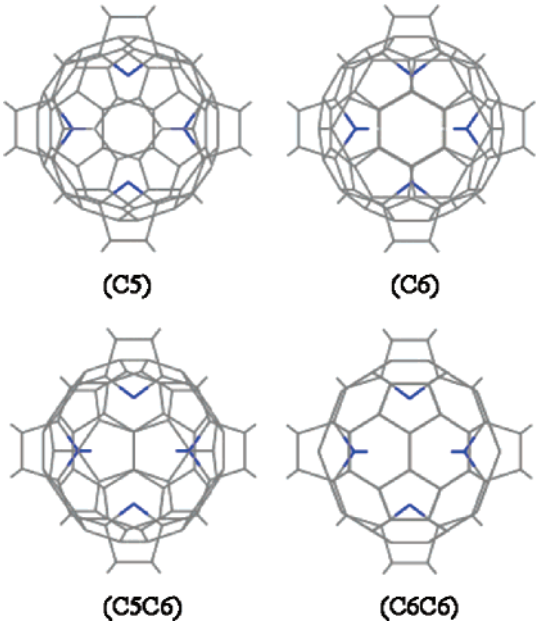

Figure 3. Different complexes of $H_2P\cdots C_{60}$ at an angle of 0°. The label texts in parentheses specify the segments of C_{60} that are closest to the molecular plane of H_2P.

Orientations and the corresponding labels of the studied $H_2P\cdots C_{60}$ complexes are presented in Figure 3. The label texts in parentheses specify the segments of C_{60} that are closest to the molecular plane of H_2P. Because fullerene is formed by hexagon rings of carbon that are surrounded by pentagon rings of carbon, the four simplest segments are pentagon (C5), hexagon (C6), pentagon−hexagon (C5C6), and hexagon−hexagon (C6C6).

The chosen electronic structure calculation method is based on the density functional theory (DFT). The main purpose of this study is to use DFT and time-dependent DFT (TDDFT) to find the transitions that lead to the experimentally observed excited states taking part in the photoinduced electron-transfer process in porphyrin−fullerene dyads. Two different types of functionals (described later) are used in calculations to study whether one or the other is more suitable for determining the transitions. To our knowledge, there is no experimental data available for nonbonded porphine−fullerene complexes. Therefore, modeling studies are used to gain insight into the interactions between porphine and fullerene at various relative orientations. The modeling results are compared to the experimental results obtained for covalently bonded porphyrin−fullerene dyads.[9,10]

II. Theoretical Methods

Geometries and electronic structures were optimized by using the density functional theory (DFT).[11−14] The ground state geometries have been determined by total energy minimization. The Becke's three-parameter hybrid-exchange functional with the Lee-Yang-Parr correlation functional (B3LYP)[15−20] and the generalized gradient approximation (GGA) type Perdew-Burke-Ernzerhof (PBE)[15,16,21,22] exchange-correlation functionals were used in calculations. All calculations were performed using the Karlsruhe split-valence basis sets[23,24] augmented with polarization functions (SVP).[25] The SVP basis set consists of three basis functions for H (4s1p)/[2s1p] and six basis functions for C and N (7s4p1d)/[3s2p1d]. All electronic excitation calculations were performed by using the time-dependent density functional theory (TDDFT).[13,26−30]

First, the geometries of H_2P and C_{60} were optimized using both functionals. The D_{2h} and I_h symmetries were used for H_2P and C_{60}, respectively. The H_2P was set onto the *xy*-plane so that its geometric center point was at the origin and the inner hydrogen atoms of two pyrrole groups were on the *x*-axis. The geometric center point of C_{60} was at the origin, and the *z*-axis was directed through the centers of the two opposite pentagon rings. These geometries were then used to construct the different $H_2P\cdots C_{60}$ complexes for both functionals by setting the H_2P onto the *xy*-plane, as described previously, and the geometric center point of fullerene on the positive *z*-axis. The starting complexes (later on labeled as a 0° complex) are presented in Figure 3. In the case of the (C5C6) and (C6C6) complexes, the fullerene was also rotated 45 and 90° clockwise with respect to the *z*-axis. The starting distance between the geometric center points of H_2P and C_{60} was set at 5.0 Å, and the optimum structure was determined. After the initial results, the final starting distance of 6.75 Å was selected for the B3LYP calculations and 6.50 Å for the PBE calculations to reduce the computational time when a higher convergence criterion was used. The complete set of coordinates is available upon request. The shape of the complexation energy curve of $H_2P\cdots C_{60}$ was studied by calculating single-point energies at different intermolecular distances between separately optimized H_2P and C_{60} structures.

Excitation energies and oscillator strengths were obtained from the TDDFT calculations. In the TDDFT theory, the electronic excitations were calculated starting from the ground state Kohn-Sham (KS) orbitals and their eigenvalues.[13] Thereafter, the electronic excitations were defined by means of the linear-response theory and by using adiabatic local density approximation (ALDA) for the functional derivatives of the exchange-correlation potential.[13] TDDFT results are proposed to be the most reliable if the excitation energy is significantly smaller than the ionization potential of the molecule (because the DFT does not predict the HOMO energy of a molecule well enough), and the one-electron excitations do not include orbitals having positive Kohn-Sham eigenvalues.[31] Both of these requirements are realized in all TDDFT results presented in this study. Only singlet states have been considered. All DFT and TDDFT calculations have been performed using the TURBOMOLE 5.7 software package.[32,33]

III. Results and Discussion

Ground State Energies and Geometries. Complexation energies, E_C, and the equilibrium interchromophore edge-to-edge distances, R_{E-E}, of different $H_2P\cdots C_{60}$ complexes are presented in Table 1. The complexation energy (E_C) is the energy of the dyad from which the energies of porphine and fullerene, which are at an infinite distance from each other, are

TABLE 1: Complexation Energies E_C and the Equilibrium Interchromophore Edge-to-Edge Distances R_{E-E} at Various Relative H_2P···C_{60} Orientations[a]

		B3LYP		PBE	
H_2P···C_{60} complex		E_C (meV)	R_{E-E} (Å)	E_C (meV)	R_{E-E} (Å)
(C5)	0°	−50	3.6	−150	3.4
(C6)	0°	−50	3.8	−150	3.4
(C5C6)	0°	−50	3.5	−140	3.4
	45°	−50	3.5	−140	3.3
	90°	−50	3.5	−170	3.1
(C6C6)	0°	−40	3.5	−120	3.4
	45°	−50	3.5	−150	3.3
	90°	−30	3.5	−140	3.1

[a] The distance between the geometric center points of H_2P and C_{60} was obtained by adding 3.3 Å to the R_{E-E} of the (C5) and (C6) complexes and 3.5 Å to the R_{E-E} of the (C5C6) and (C6C6) complexes.

subtracted, that is

$$E_C = E_{H_2P\cdots C_{60}} - (E_{H_2P} + E_{C_{60}})$$

The edge-to-edge distance is defined as a distance from the geometric center point of the plane formed by the nitrogens and carbons of the porphine ring to the center of the closest segment of fullerene. The absolute value of the magnitude of the complexation energy calculated by using B3LYP is approximately 2 times, and the corresponding value calculated by using PBE is approximately 6 times the thermal energy at room temperature (∼25 meV). This means that the PBE functional predicts a stronger interaction between H_2P and C_{60}. The maximum difference between the complexation energies (and also between the total energies) of different H_2P···C_{60} complexes is 20 meV when calculated by using B3LYP and 50 meV when calculated by using PBE. Differences between the complexation energies of different complexes calculated by using the same functional are so small that in principle all complexes are possible and equally probable. On the other hand, the complexation energies are so small that it is possible that the H_2P···C_{60} complexes would dissociate without the effect of the basis set superposition error (BSSE), which overestimates the stability of the complex. The effect of the BSSE was not studied because Shephard and Paddon-Row observed that with the B3LYP functional, the distance between H_2P and C_{60} remained the same even though the BSSE corrected complexation energy was positive.[34] However, porphyrin and fullerene form naturally assembled cocrystallates in which C_{60} is located on top of the center of the porphyrin plane and the electron-rich juncture of the (C6C6) segment is closest to the porphyrin plane.[35−37] The calculated results do not explain or support this kind of a behavior.

The geometries of the individual H_2P and C_{60} molecules in the optimized complex structures were distorted from their individual starting geometries only slightly, and the change in the mutual orientation of H_2P and C_{60} was negligible. In all complexes, the intermolecular distances calculated by using the PBE functional were shorter than those yielded by the B3LYP functional. The shortest calculated edge-to-edge distance, R_{E-E}, of 3.1 Å is found in both the (C5C6)/90°/PBE and the (C6C6)/90°/PBE complexes. In these complexes, the distance between a hydrogen atom of the pyrrolidine ring of H_2P and a carbon atom of C_{60} is the shortest. The R_{E-E} PBE values are 0.1−0.7 Å shorter than the R_{E-E} B3LYP values.

From the results presented in Table 1, it can be seen that H_2P and C_{60} have the strongest interaction in the (C5C6)/90°/PBE complex because in this structure the complexation energy is the smallest. Rotation of fullerene does not have a significant effect on the R_{E-E} (<0.1 Å) when using B3LYP but has a clear effect (∼0.3 Å) when PBE is used.

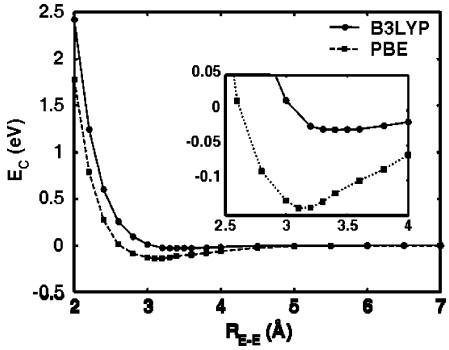

Figure 4. Graphical presentation of the B3LYP and PBE complexation energies, E_C, of the H_2P···C_{60}/(C6C6)/90° structure in which the H_2P and C_{60} geometries remain frozen at their separately optimized ground state geometries together with the corresponding equilibrium interchromophore edge-to-edge separations R_{E-E}.

The calculated edge-to-edge distances (see Table 1), R_{E-E}, are 0.1−1.1 Å longer than the experimentally observed distances of 2.7−3.0 Å in naturally assembled porphyrin−fullerene cocrystallates, in which the distance between porphyrin and fullerene is unusually short.[35,36,38,39] The PBE distances are in a better agreement with the experimental values than the B3LYP distances. Especially, the R_{E-E} of 3.1 Å in the (C6C6)/90°/PBE complex is very close to the experimental values in which the juncture of the (C6C6) segment is also nearest to the porphyrin plane, as mentioned previously. One of the two most probable reasons for the differences between the calculated and the experimental distances is that the calculated distances are for separate molecules in a vacuum, whereas the experimental distances are for cocrystallites. In cocrystallites, the equilibrium distance is smaller due to the additional attractive forces caused by the packing arrangement of the molecules.[40] The second reason is that the conventional approximations to DFT do not include the dispersive forces correctly[41−43] for nonbonded molecular structures and therefore yield incorrect interaction energies.

Basiuk[40,44] and Shephard and Paddon-Row[34] have calculated ground state properties of a H_2P···C_{60} complex by using DFT with various functionals as implemented in the DMol3 and Gaussian 98 programs, respectively, but their results relate only to the (C6C6)/90° complex. The slight distortion of the geometries of the H_2P and C_{60} molecules is consistent with Basiuk's BLYP results. The complexation energy and edge-to-edge distance calculated in our work are both in a good agreement with Shephard's B3LYP results.

The single-point complexation energies, E_C, of H_2P···C_{60}/(C6C6)/90° at different interchromophore edge-to-edge distances, R_{E-E}, calculated with B3LYP and PBE are presented in Figure 4. The results are obtained for a H_2P···C_{60} structure in which the H_2P and C_{60} structures are kept frozen at their separately optimized ground state structures, and only the distance between them is varied. From the results, it is obvious that the complexation energy, E_C, changes more strongly with the PBE than with the B3LYP functional when the R_{E-E} is changed, especially around the R_{E-E} corresponding to the minimum energy. The R_{E-E} distance that corresponds to the complexation energy minimum is 3.5 Å with B3LYP and 3.1 Å with PBE. These distances are the same as in the optimized H_2P···C_{60} structure (see Table 1), which means that the structures of H_2P and C_{60} in H_2P···C_{60} are not significantly different from the separately optimized ground state structures.

TABLE 2: Energies ϵ of Some Frontier Molecular Orbitals of the (C6C6)/90° Complex and Energies of Corresponding Orbitals of the Noninteracting[a] H_2P and C_{60} Molecules Calculated Using the HOMO Energy[b] as a Reference

	$H_2P\cdots C_{60}$/(C6C6)/90°		H_2P and C_{60}	
orbital	B3LYP ϵ (eV)	PBE ϵ (eV)	B3LYP ϵ (eV)	PBE ϵ (eV)
LUMO + 8	4.30	3.05	4.08	2.77
LUMO + 7	3.21	2.08	2.98	1.92
LUMO + 6	3.21	2.07	2.98	1.91
LUMO + 5	3.20	2.06	2.98	1.78
LUMO + 4	2.91	1.91	2.91	1.78
LUMO + 3	2.90	1.90	2.90	1.78
LUMO + 2	2.03	1.03	1.80	0.74
LUMO + 1	2.03	1.03	1.80	0.74
LUMO	2.02	1.02	1.80	0.74
HOMO	0	0	0	0
HOMO − 1	−0.16	−0.27	−0.16	−0.27
HOMO − 2	−0.69	−0.61	−0.93	−0.86
HOMO − 3	−0.70	−0.61	−0.93	−0.91
HOMO − 4	−0.70	−0.61	−0.93	−0.91
HOMO − 5	−0.71	−0.63	−0.93	−0.91
HOMO − 6	−0.71	−0.63	−0.93	−0.91
HOMO − 7	−1.20	−0.86	−1.20	−0.91
HOMO − 8	−1.33	−0.98	−1.33	−0.98

[a] The results are for H_2P and C_{60} that are 100 Å apart. The results obtained by combining the calculated energies of separate H_2P and C_{60} differ by <0.01 eV from these results. [b] The HOMO energies of $H_2P\cdots C_{60}$ are −5.37 and −5.00 eV for the B3LYP and PBE functionals, respectively. The corresponding HOMO energies of the noninteracting H_2P and C_{60} are −5.30 and −4.90 eV, respectively.

The distance R_{E-E} at which there is practically no interaction between H_2P and C_{60} (E_F < 1 meV) is ∼6.4 Å for B3LYP and ∼6.6 Å for PBE.

Ground State Electronic Structure. The B3LYP and PBE energies of some frontier orbitals of the interacting $H_2P\cdots C_{60}$/(C6C6)/90° complex and the energies of the corresponding orbitals of a complex formed by noninteracting H_2P and C_{60} are shown in Table 2. The (C6C6)/90° complex was selected as an example because it has been experimentally observed, as mentioned previously, and there are former calculations for the same structure.[34,40,44] Energy differences between the corresponding orbitals of different complexes are very small (<0.03 eV) when the same functional is used, and so only the values of one complex are shown. However, the B3LYP energies of all occupied orbitals presented in Table 2 are ca. 0.1−0.4 eV smaller and those of all unoccupied orbitals are ca. 1.0−1.3 eV larger than the PBE energies. The energies of orbitals localized to H_2P in $H_2P\cdots C_{60}$ are almost the same as the energies of the corresponding orbitals of the H_2P, whereas the energies of orbitals localized to C_{60} in the $H_2P\cdots C_{60}$ are ca. 0.2−0.3 eV larger than the energies of the corresponding orbitals in C_{60}. A HOMO−LUMO gap of 2.0 eV is obtained for $H_2P\cdots C_{60}$ with B3LYP and of 1.0 eV with PBE, whereas a ∼0.2−0.3 eV smaller HOMO−LUMO gap is obtained for the complex of noninteracting H_2P and C_{60}. The degeneracy of various orbitals of C_{60}[3,45] is also observed in our calculations on $H_2P\cdots C_{60}$.

The B3LYP orbitals of the interacting $H_2P\cdots C_{60}$ complex are approximately a combination of the orbitals of separate porphine and fullerene molecules. However, when the PBE functional is used, there is a mixing in the order of the localized orbitals when compared to the order in separate H_2P and C_{60}. For example, the HOMO − 7 orbital of the interacting $H_2P\cdots C_{60}$ complex corresponds to the HOMO − 2 orbital of the complex of noninteracting H_2P and C_{60}. Also, the LUMO + 6 and LUMO + 7 orbitals of noninteracting H_2P and C_{60} correspond to the LUMO + 3 and LUMO + 4 orbitals of the interacting $H_2P\cdots C_{60}$ complex, respectively. This is because the interaction between H_2P and C_{60} changes the orbital energies in C_{60}, whereas the energies of the H_2P orbitals remain the same. Because the energy difference between some of the orbitals of H_2P and C_{60} is small, the order of the orbitals can change.

To illustrate the differences in localization of orbitals, isoamplitude surfaces of some frontier orbitals of $H_2P\cdots C_{60}$/(C6C6)/90°/PBE are shown in Figure 5. From these orbitals, it can be seen that the electronic structure of the interacting $H_2P\cdots C_{60}$ complex is obtained roughly by combining the orbitals of H_2P and C_{60}, but because of the interaction between H_2P and C_{60}, there are changes in the localization of the orbitals (e.g., HOMO − 2 and LUMO + 7). The orbitals from HOMO − 6 to HOMO − 2 that are located mainly on C_{60} arise from the 5-fold degenerate HOMO of C_{60}.[45] The HOMO − 1 and HOMO orbitals of $H_2P\cdots C_{60}$ are located at H_2P and can be related to the HOMO − 1 and HOMO of H_2P, respectively. LUMO, LUMO + 1, and LUMO + 2 are located mainly on C_{60}, as expected, and they can be related to the triply degenerate LUMO of C_{60}.[3] The LUMO + 3 and LUMO + 4 of $H_2P\cdots C_{60}$ correspond to the LUMO and LUMO + 1 of H_2P, respectively. The orbitals from LUMO + 5 to LUMO + 7 arise from the triply degenerate LUMO + 2 of C_{60}. The shape and the degree of delocalization of orbitals depend on a complex and the functional used, but the main features (e.g., which molecule the orbital mainly belongs to) are very similar. Degeneration of fullerene orbitals is practically retained in $H_2P\cdots C_{60}$, and also, the shapes of the orbitals localized to fullerene in $H_2P\cdots C_{60}$ are roughly the same as in a single fullerene. Likewise, the shapes of the porphine orbitals and of the orbitals localized to porphine in $H_2P\cdots C_{60}$ are almost similar. The figures of orbitals of different complexes are available upon request.

Electronic Absorption Spectra. Absorption spectra of different $H_2P\cdots C_{60}$ complexes calculated with the B3LYP and PBE functionals are presented in Figures 6 and 7. In the spectra, the excitation energies and the corresponding oscillator strengths are plotted using a Gaussian distribution function with a 50 meV standard deviation. The orientation of fullerene with respect to the porphine plane has no effect on the shape of the absorption spectrum when B3LYP is used, but the shapes of the absorption spectra of different complexes differ significantly when PBE is used. The main reason for the significant shape differences in spectra is probably the stronger interaction between H_2P and C_{60} predicted by the PBE functional. This causes more changes in the energies of occupied and unoccupied orbitals in different $H_2P\cdots C_{60}$ complexes. For a detailed study, the excited states, excitation energies, oscillator strengths, and dominating one-electron excitations of the (C6C6)/90° complex calculated by using the B3LYP and PBE functionals are given in Table 3. Corresponding dominant one-electron excitations of other complexes (available upon request) are similar in principle, but excitation energies and oscillator strengths of different complexes differ, especially when calculated with the PBE functional.

The interaction between porphine and fullerene is seen when the excitation energies of the interacting $H_2P\cdots C_{60}$ complex and of the noninteracting H_2P and C_{60} are compared. For this purpose, the calculated TDDFT/B3LYP and TDDFT/PBE excitation energies, oscillator strengths, and dominant one-electron excitations of the lowest two transitions of noninteracting H_2P and C_{60} are presented in Table 4. It can be seen that in the spectrum of $H_2P\cdots C_{60}$, there exist transitions that have energies lower than the energies of the lowest transitions in

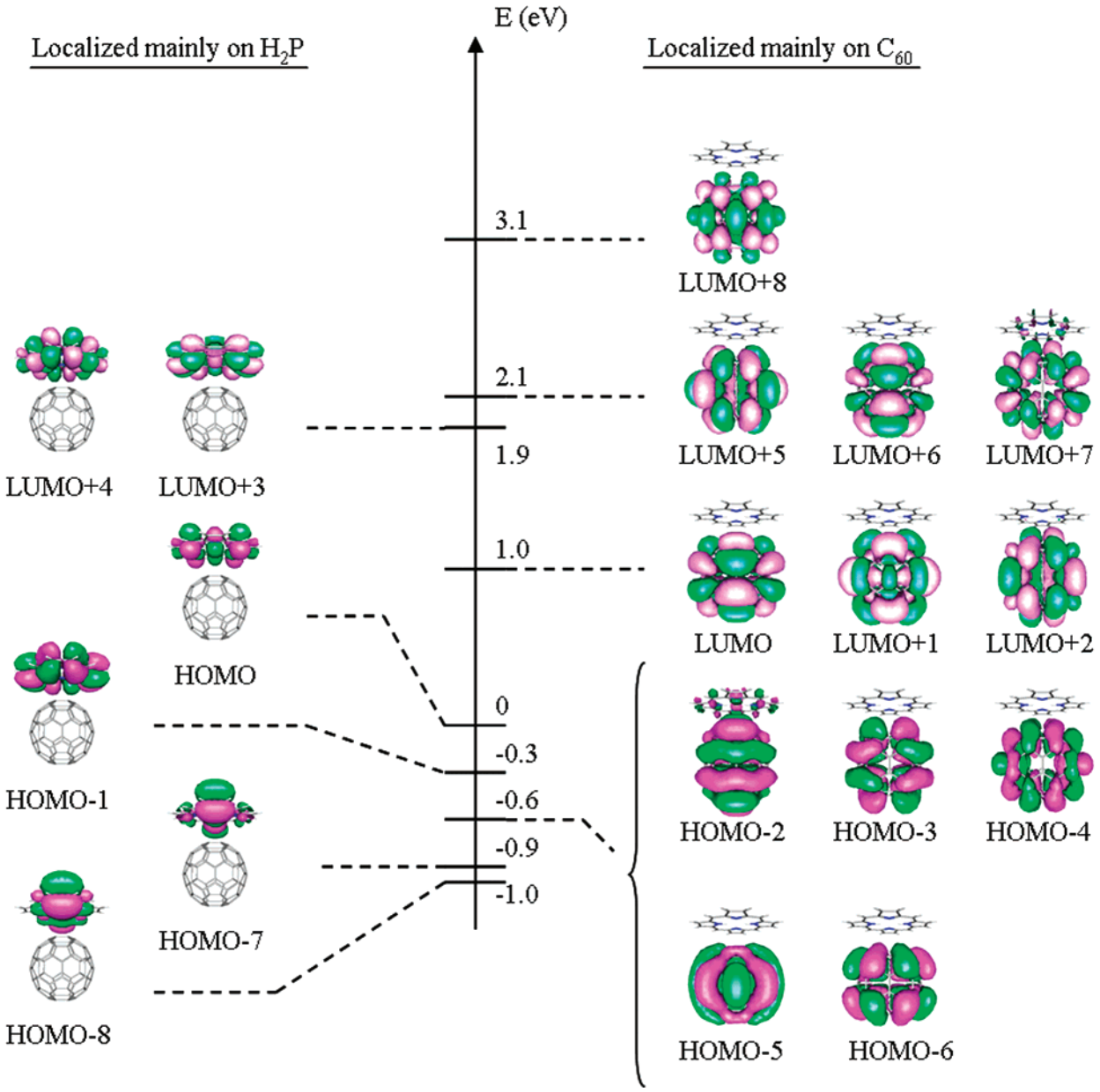

Figure 5. Some of the frontier orbitals and corresponding orbital energies yielded by the PBE functional for H_2P···C_{60}/(C6C6)/90°. The energies are given relative to the HOMO energy of −5.00 eV. The isoamplitude surfaces of the orbitals presented are 10% of the maximum positive (green) and minimum negative (red) values of the wave functions.

either H_2P or C_{60} and are a consequence of the interaction between H_2P and C_{60}.

The one-electron excitations of electronic transitions are analyzed, and the results are used to designate the excited states (ES) involved in an electron-transfer process of a porphyrin−fullerene dyad (see Figure 1). The excited states and the corresponding one-electron transitions of H_2P···C_{60}/(C6C6)/90° are listed in Table 3. Three different types of excited states can be identified on the basis of their one-electron excitations (see Table 3). They are in the order of increasing energy: (1) the excited charge-transfer complex state ((PC)*), (2) the locally excited fullerene state (PC^{1S}), and (3) the locally excited porphine state (($P^{1S}C$) and ($P^{2S}C$)). All these states except the locally excited fullerene state are also observed in experimental studies.[9] These states are analyzed next.

Excited Charge-Transfer Complex State. Charge transfer can take place from porphine to fullerene when the molecules are in close proximity and form a ground state complex like in this study. The excited charge-transfer complex state ((PC)*) is identified on the basis of the localization of the orbitals that take part in transition. In addition, the nature of the (PC)* is defined by the contribution of the charge transfer from H_2P to C_{60}. In other words, if the (PC)* has a dominant contribution of a radical ion-pair nature ($P^{\bullet+}C^{\bullet-}$), the transition should be from an orbital localized on H_2P to an orbital localized on C_{60}, and (PC)* can be regarded as a contact radical ion pair.[46] The observed low energy absorption bands (<2 eV by B3LYP and <1.5 eV by PBE) cannot be related to either absorption of H_2P or absorption of C_{60} but can be regarded as charge-transfer complex absorption bands (because of the nonzero dipole moment from C_{60} to H_2P in the ground state). This means that existence of a linker between porphyrin and fullerene is not a prerequisite for the formation of an excited charge-transfer complex state.

The dominating one-electron excitations of different transitions presented in Table 3 for the (C6C6)/90° complex are very similar to those in other complexes calculated by using the same functional. Transitions 1−3 are from HOMO to LUMO, LUMO

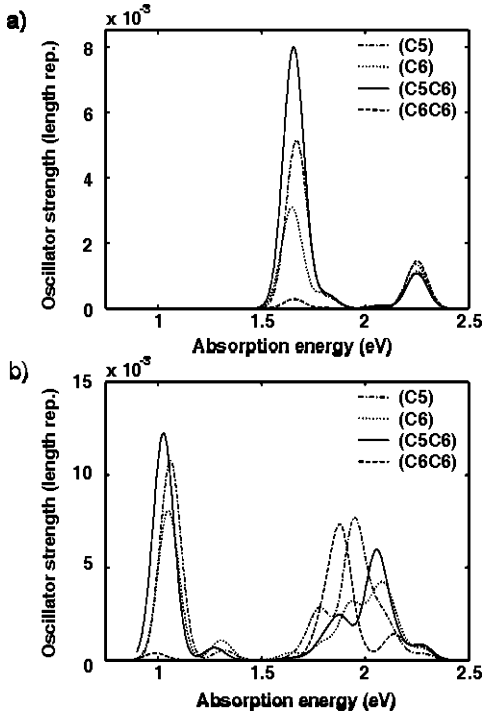

Figure 6. Absorption spectra of different $H_2P\cdots C_{60}$ complexes at an angle of 0° calculated using the (a) B3LYP and (b) PBE functionals.

+ 1, or LUMO + 2, in other words, from H_2P to C_{60}. Also, transitions 4−6 are from H_2P to C_{60} but are from HOMO − 1 to LUMO, LUMO + 1, or LUMO + 2. Transitions 1−3 and 4−6 are almost degenerate, which is a consequence of the nearly degenerate LUMO, LUMO + 1, and LUMO + 2 states of $H_2P\cdots C_{60}$ as mentioned previously. We consider that all these six lowest excitations lead to the excited charge-transfer complex states, which can be regarded as contact radical ion pairs. The transition energies of the (PC)* states are 1.6−1.9 eV when calculated with B3LYP and 1.0−1.3 eV when calculated with PBE.

In our work, the B3LYP results are in a good agreement with the experimental observations for a covalently linked porphyrin−fullerene dyad in which the absorption energy of the charge-transfer complex state is ∼1.65−1.77 eV.[9,10] The PBE energies, however, are underestimated by ∼0.3−0.8 eV if compared to the experimental results. The excitations corresponding to the PBE-calculated transitions 22−30 are not seen in the B3LYP results but are expected at excitation energies higher than the excitation energy of ($P^{2S}C$). The PBE transitions 22−30 are from orbitals localized on porphine to fullerene and also can be considered to lead to an excited charge-transfer complex. A mixing of the states of the locally excited porphine and the radical ion pair is seen in transition 29. In several studies, TDDFT has been found to inaccurately describe the excitation energies of charge-transfer excited states.[47−51] It has been observed that the hybrid type B3LYP functional describes the charge-transfer better than the local GGA type PBE functional,[49] which also is supported by this study, as shown previously.

It is possible that the excited charge-transfer complex state proceeds to a complete charge-separated state. The electron has to move from a donor (porphine) to an acceptor (fullerene) before the complete charge-separated state is formed. In the simplest case, this would correspond to a transition from HOMO to LUMO (or to LUMO + 1 or to LUMO + 2 because of the degeneration), and for the system studied here, it corresponds to the transitions 1−3. To be able to define the transition that would produce a complete charge-separated state among these similar transitions, one would need information, for example, on excited state dipole moments. This would mean an optimization of an excited state structure, which is not performed when calculating electronic transitions with the present TDDFT approach.

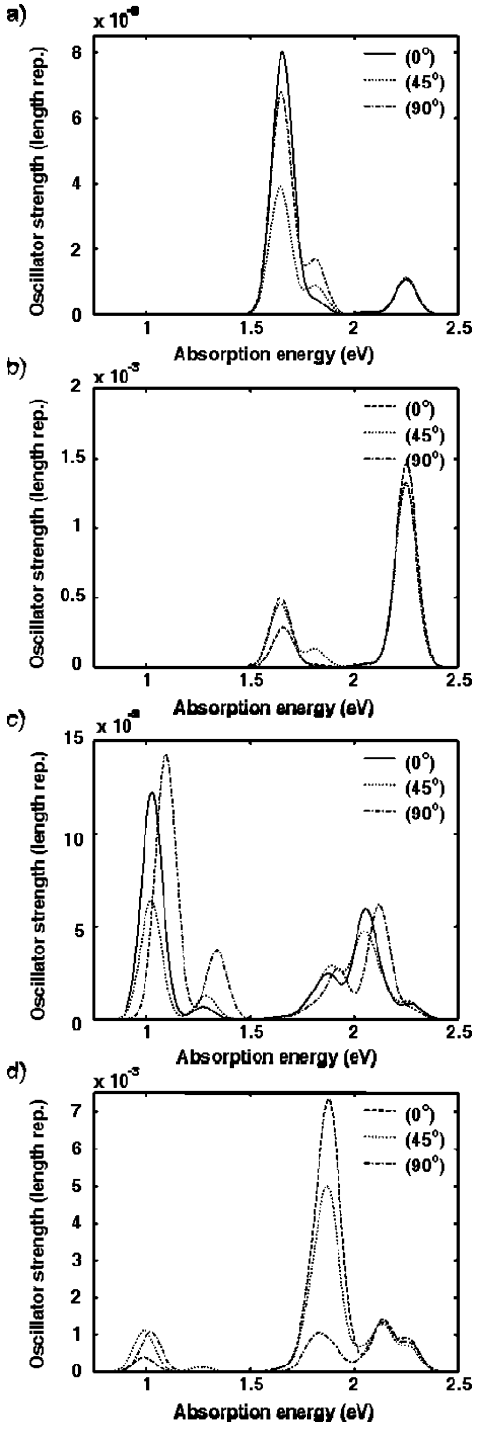

Figure 7. Absorption spectra of $H_2P\cdots C_{60}$ (a) (C5C6) and (b) (C6C6) complexes yielded by the B3LYP functional and of (c) (C5C6) and (d) (C6C6) complexes yielded by the PBE functional at three different C_{60} rotational angles.

Locally Excited Fullerene and Porphine States. Transitions producing locally excited states of fullerene (porphine) should only take place between orbitals localized mainly on fullerene (porphine). All transitions 7−21 in Table 3 are from orbitals localized fully or mainly on fullerene to orbitals localized fully on fullerene. The corresponding transition energies are 2.0−

TABLE 3: TDDFT Calculated Electronic Transitions (TR), Excited States (ES), Excitation Energies (*E*), Oscillator Strengths[a] (*f*), and Corresponding One-Electron Excitations and Their Weights for the H_2P···C_{60}/(C6C6)/90° Complex[b,c]

	TDDFT/B3LYP				TDDFT/PBE			
TR	ES	*E* (eV)	f ($\times 10^{-3}$)	one-electron excitation and weight	ES	*E* (eV)	f ($\times 10^{-3}$)	one-electron excitation and weight
1	(PC)*	1.63	~0	H → L + 2 58%; H → L + 1 41%	(PC)*	1.02	1	H → L 100%
2		1.63	~0	H → L + 1 58%; H → L + 2 41%		1.03	~0	H → L + 1100%
3		1.65	0.5	H → L 100%		1.03	~0	H → L + 2100%
4		1.81	~0	H − 1 → L + 1 99%		1.29	~0	H − 1 → L 100%
5		1.81	~0	H − 1 → L + 2 99%		1.30	~0	H − 1 → L + 1100%
6		1.82	~0	H − 1 → L 100%		1.31	~0	H → L + 2100%
7	PC^{1S}	2.06	~0	H − 4 → L 79%	PC^{1S}	1.66	0.01	H − 2 → L 42%; H − 4 → L + 2 31%; H − 5 → L + 1 27%
8		2.06	~0	H − 2 → L 34%; H − 4 → L + 2 23%; H − 5 → L + 1 18%		1.66	~0	H − 2 → L + 1 55%; H − 3 → L + 2 32%; H − 6 → L + 2 11%
9		2.06	~0	H − 3 → L 50%; H − 6 → L 16%		1.66	~0	H − 4 → L 67%; H − 6 → L + 1 29%
10		2.06	~0	H − 2 → L + 1 50%; H − 3 → L + 2 26%		1.66	~0	H − 3 → L 55%; H − 5 → L + 2 30%; H − 6 → L 15%
11		2.07	~0	H − 2 → L + 2 71%; H − 3 → L + 1 22%		1.70	~0	H − 3 → L + 2 54%; H − 2 → L + 1 28%; H − 5 → L 18%
12		2.08	~0	H − 3 → L + 2 60%; H − 2 → L + 1 26%		1.71	~0	H − 6 → L + 1 45%; H − 2 → L + 2 45%
13		2.08	~0	H − 4 → L + 1 73%; H − 6 → L 14%		1.71	~0	H − 4 → L + 1 56%; H − 5 → L + 2 29%
14		2.08	~0	H − 5 → L 78%; H − 6 → L + 2 17%		1.72	~0	H − 3 → L + 1 40%; H − 2 → L + 2 37%; H − 6 → L + 1 13%
15		2.08	~0	H − 6 → L + 1 70%; H − 3 → L + 1 12%		1.73	~0	H − 6 → L 52%; H − 4 → L + 1 27%; H − 5 → L + 2 20%
16		2.09	~0	H − 5 → L + 2 54%; H − 6 → L 40%		1.73	~0	H − 5 → L 68%; H − 6 → L + 2 15%; H − 3 → L + 2 12%
17		2.24	~0	H − 2 → L 58%; H − 4 → L + 2 32%		1.79	0.02	H − 2 → L 55%; H − 4 → L + 2 34%
18		2.25	0.8	H − 3 → L + 1 51%; H − 4 → L 15%; H − 2 → L + 2 13%; H − 6 → L + 1 11%		1.80	0.5	H − 3 → L + 1 56%; H − 4 → L 15%; H − 2 → L + 2 14%; H − 6 → L + 1 13%
19		2.25	~0	H − 3 → L 37%; H − 6 → L 26%; H − 5 → L + 2 17%; H − 4 → L + 1 15%		1.81	~0	H − 3 → L 34%; H − 6 → L 27%; H − 5 → L + 2 21%; H − 4 → L + 1 16%
20		2.26	0.07	H − 5 → L + 1 59%; H − 4 → L + 2 29%		1.81	0.1	H − 5 → L + 1 63%; H − 4 → L + 2 34%
21		2.26	0.4	H − 6 → L + 2 63%; H − 5 → L 15%; H − 2 → L + 1 13%		1.82	0.3	H − 6 → L + 2 73%; H − 5 → L 13%; H − 2 → L + 1 11%
22	P^{1S} C	2.27	0.02	H → L + 4 59%; H − 1 → L + 3 40%	(PC) *	1.88	~0	H − 7 → L 100%
23	P^{2S} C	2.43	~0	H → L + 3 55%; H − 1 → L + 4 44%		1.89	0.6	H − 7 → L + 1 100%
24						1.89	~0	H − 7 → L + 2 100%
25						2.00	0.06	H − 8 → L 100%
26						2.01	0.04	H − 8 → L + 1 100%
27						2.01	~0	H − 8 → L + 2 100%
28						2.06	~0	H → L + 5 100%
29						2.07	0.2	H → L + 7 87%; H → L + 4 11%
30						2.07	0.04	H → L + 6 99%
31					$P^{1S}C$	2.14	1	H → L + 4 55%; H − 1 → L + 3 32%; H → L + 7 12%
32					$P^{2S}C$	2.26	0.8	H → L + 3 59%; H − 1 → L + 4 37%

[a] Oscillator strengths are length representations, and all oscillator strengths smaller than 10^{-5} are marked as ~0. [b] Only the one-electron excitations contributing more than 10% to a particular transition are included. [c] The corresponding absorption spectra are shown in Figure 7b,d.

TABLE 4: TDDFT Calculated Lowest Two Electronic Transitions (TR), Excitation Energies (*E*), Oscillator Strengths[a] (*f*), and Corresponding One-Electron excitations of H_2P and C_{60}[b]

		TDD FT/B3LYP			TDDFT/PBE		
	TR	*E* (eV)	f ($\times 10^{-6}$)	one-electron excitation and weight	*E* (eV)	f ($\times 10^{-6}$)	one-electron excitation and weight
H_2P[c]	1b3u	2.27	70	H → L + 1 59%; H − 1 → L 40%	2.14	2×10^3	H → L + 1 64%; H − 1 → L 35%
	1b2u	2.43	4	H → L 55%; H − 1 → L + 1 45%	2.28	10^3	H → L 59%; H − 1 → L + 1 40%
C_{60}	1t1u	3.44	0.03×10^6	H → L + 1 79%; H − 2 → L 20%	2.77	5×10^3	H → L + 1 70%; H − 2 → L 30%
	2t1u	3.90	0.5×10^6	H − 2 → L 61%; H → L + 3 25%; H → L + 1 11%	3.43	0.3×10^6	H − 2 → L 48%; H → L + 3 32%; H → L + 1 18%

[a] Oscillator strengths are length representations. [b] Only the one-electron excitations contributing more than 10% to a particular transition are included. [c] The H_2P B3LYP results are the same as the results presented in ref 28 for the same type of calculation.

2.3 eV (B3LYP) and 1.6−1.9 eV (PBE). These transitions correspond to a locally excited fullerene state (PC^{1S}), but because the excitation energies are much smaller than the calculated excitation energy of the first transition of fullerene (B3LYP: 3.44 eV and PBE: 2.77 eV), the identification of the actual PC^{1S} state using these values as a reference is not possible. The observed decrease of the excitation energy is noticeable because for noninteracting H_2P and C_{60}, the excitation energy to the first excited state of C_{60} is higher than the energy of the first excited state of H_2P, but for locally excited states of H_2P···C_{60}, the energy order is the opposite. This is an unexpected result, especially for B3LYP, because as was mentioned earlier, the energies of the ground state orbitals of a complex are approximately the sums of the energies of the orbitals of separate porphine and fullerene molecules.

From the experimental absorption spectrum of a covalently linked porphyrin−fullerene dyad, the absorption of the locally excited fullerene is hard to identify because porphyrin absorbs more strongly at energies <3.1 eV.[7,9,52] Likewise, a comparison to an experimental absorption spectrum of fullerene is not useful for defining the locally excited state of fullerene. This is because fullerene has characteristic absorption peaks at energies of ~5.8,

~4.8, and ~3.8 eV and a less intensive absorption at ~3.1 eV.[53−55] These energies are much higher than the calculated B3LYP and PBE energies of the PC^{1S} state (2.0−2.3 and 1.6−1.9 eV, respectively).

The transitions 22 and 23 of all complexes calculated by using B3LYP correspond to the first two lowest transitions, which form the locally excited singlet states of porphyrin, $P^{1S}C$, and $P^{2S}C$, respectively. The excitation energy is 2.27 eV for $P^{1S}C$ and 2.43 eV for $P^{2S}C$. The PBE transitions 31 and 32 of all complexes correspond to the $P^{1S}C$ and $P^{2S}C$ states, respectively. The PBE transition energy of $P^{1S}C$ is 2.14 eV and of $P^{2S}C$ 2.26 eV. These values correspond to the calculated first and second excitation energies of H_2P, and the dominating one-electron excitations are very similar in all $H_2P\cdots C_{60}$ complexes when the same functional is used. The B3LYP and PBE excitation energies to the $P^{1S}C$ and $P^{2S}C$ excited states are close to the experimental excitation energies of H_2P (i.e., 1.98−2.02 eV for the H_2P^{1S} state and 2.33−2.42 eV for the H_2P^{2S} state).[5,56,57]

The PBE functional gives more such transitions that have energies lower than the energy of the locally excited state of porphine. This is understandable because B3LYP and PBE yield different orbital energies. Magnitudes of the calculated oscillator strengths of different states related to the photoinduced charge-transfer complex reactions are of about the same order, which is not consistent with the experimental results for a covalently linked porphyrin−fullerene dyad, in which the oscillator strength of the excited charge-transfer complex is about 2 orders smaller than oscillator strengths of locally excited states of porphyrin.[9]

IV. Conclusion

The spectroscopic properties of a ground state nonbonded porphine−buckminsterfullerene complex at eight different relative orientations have been studied with DFT and TDDFT by using the B3LYP and PBE functionals. The orientation of C_{60} with respect to H_2P has been found to affect the equilibrium distance between H_2P and C_{60}, especially when calculated with PBE. The excitation energies of different complexes have been found to be practically the same when the B3LYP functional is used but to differ notably when PBE is used. The changes observed with PBE are most probably due to a shorter interchromophore distance between H_2P and C_{60}. The excited charge-transfer complex state ((PC)*), the locally excited fullerene state (PC^{1S}), and the locally excited states of porphine (i.e., ($P^{1S}C$) and ($P^{2S}C$)) have been found for all complexes with both functionals. The one-electron excitations of corresponding transitions calculated by using B3LYP and PBE are mostly similar, but the excitation energies are different. The excitation energy of the excited charge-transfer complex state is within ranges of 1.6−1.9 eV (B3LYP) and 1.0−1.3 eV (PBE). The locally excited state of fullerene has an excitation energy of 2.0−2.3 eV (B3LYP) and 1.6−1.9 eV (PBE). The excitation energies corresponding to the first and second excited states of porphine are ~2.3 and ~2.4 eV with the B3LYP functional and ~2.1 and ~2.3 eV with the PBE functional, respectively.

Acknowledgment. The authors acknowledge the financial support from the Academy of Finland and the computing resources provided by the Finnish IT center for Science (CSC), Espoo, Finland. People in the research group at the Institute of Materials Chemistry, Tampere University of Technology, Finland, are acknowledged for extensive discussions related to the photoinduced electron transfer in porphyrin − fullerene based molecules.

References and Notes

(1) Kroto, H. W.; Health, J. R.; O'Brien, S. C.; Curl, R. F.; Smalley, R. E. *Nature* **1985**, *318*, 162.
(2) Kratschmer, W.; Lamb, L. D.; Fostiropoulos, K.; Huffman, D. R. *Nature* **1990**, *347*, 354.
(3) Haddon, R. C.; Brus, L. E.; Raghavachari, K. *Chem. Phys. Lett*. **1986**, *125*, 459.
(4) Imahori, H.; Hagiwara, K.; Akiyama, T.; Aoki, M.; Taniguchi, S.; Okada, T.; Shirakawa, M.; Sakata Y. *Chem. Phys. Lett*. **1996**, *263*, 545.
(5) Edwards, L.; Dolphin, H.; Gouterman, M.; Adler, A. D. *J. Mol. Spectrosc*. **1971**, *38*, 16.
(6) Imahori, H.; Hagiwara, K.; Aoki, M.; Akiyama, T.; Taniguchi, S.; Okada, T.; Shirakawa, M.; Sakata, Y. *J. Am. Chem. Soc*. **1996**, *118*, 11771.
(7) Kuciauskas, D.; Lin, S.; Seely, G. R.; Moore, A. L.; Moore, T. A.; Gust, D.; Drovetskaya, T.; Reed, C. A.; Boyd, P. D. W. *J. Phys. Chem*. **1996**, *100*, 15926.
(8) Kesti, T. J.; Tkachenko, N. V.; Vehmanen, V.; Yamada, H.; Imahori, H.; Fukuzumi, S.; Lemmetyinen, H. *J. Am. Chem. Soc*. **2002**, *124*, 8067.
(9) Vehmanen, V.; Tkachenko, N. V.; Imahori, H.; Fukuzumi, S.; Lemmetyinen, H. *Spectrochim. Acta, Part A* **2001**, *57*, 2229.
(10) Imahori, H.; Tkachenko, N. V.; Vehmanen, V.; Tamaki, K.; Lemmetyinen, H.; Sakata, Y.; Fukuzumi, S. *J. Phys. Chem. A* **2001**, *105*, 1750.
(11) Kohn, W.; Sham, L. *Phys. Rev. A: At., Mol., Opt. Phys.* **1965**, *140*, 1133.
(12) Hohenberg, P.; Kohn, W. *Phys. Rev. B: Condens. Matter* **1964**, *136*, 864.
(13) Seminario, J. M. *Recent Developments and Applications of Modern Density Functional Theory*; Elsevier: Amsterdam, 1996.
(14) Koch, W.; Holthausen, M. C. *A Chemist's Guide to Density Functional Theory*, 2nd ed.; Wiley VCH: Weinheim, 2001.
(15) Dirac, P. A. M.; *Proc. R. Soc. London, Ser. A* **1929**, *123*, 714.
(16) Slater, J. C. *Phys. Rev*. **1951**, *81*, 385.
(17) Vosko, S. H.; Wilk, L.; Nusair, M. *Can. J. Phys*. **1980**, *58*, 1200.
(18) Lee, C.; Yang, W.; Parr, R. G. *Phys. Rev. B: Condens. Matter* **1988**, *37*, 785.
(19) Becke, A. D. *Phys. Rev. A: At., Mol., Opt. Phys.* **1988**, *38*, 3098.
(20) Becke, A. D. *J. Chem. Phys*. **1993**, *98*, 5648.
(21) Perdew, J. P.; Wang, Y. *Phys. Rev. B: Condens. Matter* **1992**, *45*, 13244.
(22) Perdew, J. P.; Burke, K.; Ernzerhof, M. *Phys. Rev. Lett*. **1996**, *77*, 3865.
(23) Schäfer, A.; Horn, H.; Ahlrichs, R. *J. Chem. Phys*. **1992**, *97*, 2571.
(24) Schäfer, A.; Huber, C.; Ahlrichs, R. *J. Chem. Phys.* **1994**, *100*, 5829.
(25) Dunning, T. H., Jr. *J. Chem. Phys*. **1989**, *90*, 1007.
(26) Gross, E. K. U.; Kohn, W. *Adv. Quantum Chem*. **1990**, *21*, 255.
(27) Petersilka, M.; Grossmann, U. J.; Gross, E. K. U. *Phys. Rev. Lett*. **1996**, *76*, 1212.
(28) Bauernschmitt, R.; Ahlrichs, R. *Chem. Phys. Lett*. **1996**, *256*, 454.
(29) Bauernschmitt, R.; Häser, M.; Treutler, O.; Ahlrichs, R. *Chem. Phys. Lett*. **1997**, *264*, 573.
(30) Stratmann, R. E.; Scuseria, G. E.; Frisch, M. J. *J. Chem. Phys*. **1998**, *109*, 8218.
(31) Casida, M. E.; Casida, K. C.; Salahub, D. R. *Int. J. Quantum Chem*. **1998**, *70*, 933.
(32) Ahlrichs, R.; Bär, M.; Häser, M.; Horn, H.; Kälmel, C. *Chem. Phys. Lett*. **1989**, *162*, 165.
(33) Treutler, O.; Ahlrichs, R. *J. Chem. Phys*. **1995**, *102*, 346.
(34) Shephard, M. J.; Paddon-Row, M. N. *J. Porphyrins Phthalocyanines* **2002**, *6*, 783.
(35) Olmstead, M. M.; Costa, D. A.; Maitra, K.; Noll, B. C.; Phillips, S. L.; Van Calcar, P. M.; Balch, A. L. *J. Am. Chem. Soc*. **1999**, *121*, 7090.
(36) Boyd, P. D. W.; Hodgson, M. C.; Richard, C. E. F.; Oliver, A. G.; Chaker, L.; Brothers, P. J.; Bolskar, R. D.; Tham, F. S.; Reed, C. A. *J. Am. Chem. Soc*. **1999**, *121*, 10487.
(37) Sun, D.; Tham, F. S.; Reed, C. A.; Chaker, L.; Boyd, P. D. W. *J. Am. Chem. Soc*. **2002**, *124*, 6604.
(38) Sun, Y.; Drovetskaya, T.; Bolskar, R. D.; Bau, R.; Boyd, P. D. W.; Reed, C. A. *J. Org. Chem*. **1997**, *62*, 3642.
(39) Guldi, D. M.; Luo, C.; Prato, M.; Troisi, A.; Zerbetto, F.; Scheloske, M.; Dietel, E.; Bauer, W.; Hirsch, A. *J. Am. Chem. Soc*. **2001**, *123*, 9166.
(40) Basiuk, V. A. *J. Phys. Chem. A* **2005**, *109*, 3704.
(41) Tsuzuki, S.; Luthi, H. P. *J. Chem. Phys*. **2001**, *114*, 3949.
(42) Wu, X.; Vargas, M. C.; Nayak, S.; Lotrich, V.; Scoles, G. *J. Chem. Phys.* **2001**, *115*, 8748.
(43) van Mourik, T.; Gdanitz, R. J. *J. Chem. Phys*. **2002** *116*, 9620.
(44) Basiuk, V. A. *J. Comput. Theor. Nanosci*. **2005**, *2*, 370.
(45) Green, W. H., Jr.; Gorun, S. M.; Fitzgerald, G.; Fowler, P. W.; Ceulemans, A.; Titeca, B. C. *J. Phys. Chem*. **1996**, *100*, 14892.
(46) Gould, I. R.; Young, R. H.; Mueller, L. J.; Farid, S. *J. Am. Chem. Soc*. **1994**, *116*, 8176.

(47) Tozer, D. J.; Amos, R. D.; Handy, N. C.; Roos, B. O.; Serrano-Andres, L. *Mol. Phys.* **1999**, *97*, 859.

(48) Dreuw, A.; Weisman, J. L.; Head-Gordon, M. *J. Chem. Phys.* **2003**, *119*, 2943.

(49) Tozer, D. J. *J. Chem. Phys.* **2003**, *119*, 12697.

(50) Dreuw, A.; Head-Gordon, M. *J. Am. Chem. Soc.* **2004**, *126*, 4007.

(51) Gritsenko, O.; Baerends, E. J. *J. Chem. Phys.* **2004**, *121*, 655.

(52) Schuster, S. I.; Cheng, P.; Jarowski, P. D.; Guldi, D. M.; Luo, C.; Echegoyen, L.; Pyo, S.; Holzwarth, A. R.; Braslavsky, S. E.; Williams, R. M.; Klihm, G. *J. Am. Chem. Soc.* **2004**, *126*, 7257.

(53) Bensasson, R. V.; Bienvenue, E.; Dellinger, M.; Leach, S.; Seta, P. *J. Phys. Chem.* **1994**, *98*, 3492.

(54) Bauernschmitt, R.; Ahlrichs, R.; Hennrich, F. H.; Kappes, M. M. *J. Am. Chem. Soc.* **1998**, *120*, 5052.

(55) Guldi, D. M.; Prato, M. *Acc. Chem. Res.* **2000**, *33*, 695.

(56) Kim, B. F.; Bohandy, J. *J. Mol. Spectrosc.* **1978**, *73*, 332.

(57) Dalton, J.; Milgrom, L. R.; Pemberton, S. M. *J. Chem. Soc., Perkin Trans. 2* **1980**, *2*, 370.